Proceedings of the SPIE Symposium on Astronomical Telescopes and Instrumentation, 20 – 28 March, 1998, Kona, Hawaii.

Metrology for the Adaptive Optics System

at the Palomar 200" Telescope

E. E. Bloemhof and R. G. Dekany

Palomar Observatory and Jet Propulsion Laboratory California Institute of Technology Pasadena, CA 91125

#### ABSTRACT

Precise registration of telescope pupil, wavefront sensor camera, and science camera is critical to optimum performance of an adaptive optics system. For this reason great care is taken in design and construction to ensure optical rigidity and stability. However, some residual flexure is unavoidable, particularly for a system like the one being built at the Jet Propulsion Lab for the Cassegrain focus of the Palomar 200", which will experience changing gravity loads as the telescope points and guides. Such flexure has direct impact when it occurs in the non-common-path segments of the wavefront-sensor and science beams. The diffraction-limited image size in K-band at the 5 m telescope is 30 microns. To maintain non-common-path flexure errors at a small fraction of this scale would require costly, gravity-compensated optomechanics. A more practical approach is to use precise measurements of the flexure in a periodic recalibration of the wavefront sensor offsets. As an alternative to mapping flexure over a grid of sky pointing positions, we have investigated a low-bandwidth metrology scheme in which we sense tilts and translations of optical components in the various light paths using visible laser signals. We find that such a system is relatively easy to implement, and can be expected to provide dramatic improvement in adaptive optics performance when the "real-world" effects of telescope orientation are considered.

KEYWORDS: adaptive optics, astronomy, metrology

# 1. INTRODUCTION: ADAPTIVE OPTICS

With recent technological advances, it has become feasible to implement real-time corrections in hardware that compensate for wavefront distortions induced by the turbulent atmosphere, as first proposed by Babcock<sup>1</sup> in 1953. A number of groups are working to build such adaptive optics systems for large astronomical telescopes, and some have already made astrophysical observations of real value<sup>2</sup>. The promise of this approach is very great, particularly when combined with the new generation of large ground-based apertures that have been made possible by recent revolutionary breakthroughs in telescope manufacture.

At Palomar, an adaptive optics system for the 200" telescope has been designed and is now being built and tested by a group at the Jet Propulsion Lab<sup>3</sup>. Work has been underway for just over three years now, and the system is expected to be commissioned late in 1998. When operational, this system will provide a substantial performance boost to a telescope that remains one of the largest optical collecting areas on earth. The essential nature of the performance improvement is a substantial reduction in the scale of the point-spread function, and this has the unfortunate implication that mechanical flexures in the optical path have a proportionately larger effect. The measurement and compensation of these flexures form the subject of this paper.

## 2. THE ADAPTIVE OPTICS DESIGN FOR THE PALOMAR 200" TELESCOPE

In most respects the overall design concept of the adaptive optics system for the Palomar 200" telescope is fairly standard. The wavefront sensor is of the Shack-Hartmann type, with a  $16\times16$  lenslet array of subapertures mapped onto the diameter of the telescope primary. The deformable mirror has 349 electrostrictive PMN actuators, and 241 of these actuators map onto the telescope pupil. Some of the rest form a "guard band" around the periphery, as they are slaved to the outermost active elements, and some fall onto the central obscuration due to the secondary mirror, which is quite large at Palomar (fractional linear obscuration  $\sim 0.36$ ). Each actuator has a mechanical travel or throw of  $\sim 5~\mu m$ , giving twice that amount of total amplitude in wavefront correction capability. Wavefront sensing is done at visible wavelengths to correct a science beam in the near infrared, so that detailed information about the atmosphere can be measured but then this information is applied in a wavelength regime where the atmospheric fluctuations are slower, smaller in amplitude, and more easily corrected.

The detailed optical layout of the adaptive optics system is shown in Figure 1. The system is mounted at the f/15.7 Cassegrain focus. Most of the optical components are arranged on a custom Newport RS4000 optical bench measuring  $78"\times54"$  and 8.375" thick. Light from the telescope enters from the direction perpendicular to the plane of the diagram and is directed by the fold mirror, FM1, onto an off-axis paraboloid, OAP1. Just above FM1, on a second, smaller optical platform not shown in Figure 1, is a set of calibration optics known as the "stimulus". The stimulus provides a means of injecting a test beam that simulates a stellar source viewed through the 200" telescope into the adaptive optics system proper. In addition, a phase-shifting interferometer is positioned to view the elements of the adaptive optics system, to aid in their alignment, and an artificial generator of air turbulence can be used to test system performance. The collimated beam from OAP1 is directed onto a fast-steering mirror (FSM), which applies tip-tilt corrections at a rapid rate ( $\sim75$  Hertz); although tip-tilt could in principle be corrected by the deformable mirror, the large amplitudes found under typical atmospheric seeing conditions would overwhelm the modest throw of the deformable mirror actuators. (Similarly, the adaptive optics system will off-load corrections for the misfocus term of atmospheric seeing by updating the focus of the telescope itself on timescales of a few minutes).

From the FSM, the collimated beam travels to the deformable mirror (DM) and then on to a second off-axis paraboloid (OAP2), by way of a fold mirror (FM2) whose presence is required to package the system into the restricted space at the Cassegrain focus. The deformable mirror, of course, is charged with correcting all the higher-order distortions in the corrupted plane wave incident from a natural guide star. The converging beam from OAP2 next hits an infrared-transmitting dichroic (SSM1), which passes near-infrared (J, H, K band) radiation to the science camera (SCI CAM in Figure 1), by way of fold mirror FM3, while reflecting visible light to SSM2 and then into the wavefront sensor (WFS). The visible beam from a 4"×4" square spot on the field stop (FS) is reflected into the wavefront sensor. Light from the rest of the field is transmitted through the field stop substrate and is imaged in an acquisition camera (ACQ CAM). The acquisition camera effectively provides a  $480\times512$  array of  $11\times13~\mu m$  pixels; the beam from the sky is adapted to  $\sim f/2$  by a special Nikon lens mounted immediately in front of this camera (not shown in Figure 1, but shown quite schematically in Figures 2 and 3). Some essential parameters characterizing the various cameras in use on the Palomar AO system are summarized in Table 1.

TABLE 1
CAMERA PARAMETERS for the PALOMAR ADAPTIVE OPTICS SYSTEM

Camera	Wavelength $(\mu \mathrm{m})$	Format	$\begin{array}{c} \text{Pixel Size} \\ (\mu\text{m}) \end{array}$	Plate Scale ("/mm)	Comments
Science camera	~ 1 - 2.5	$1024 \times 1024$	18.5	2.62	J, H, K infrared bands
WFS camera	visible	$64 \times 64$	24.0	$\sim 40$	Fast (500 Hz), low read noise ( $\sim$ 7 e <sup>-</sup> )
Acquisition camera $^a$	visible	$480\times512$	$11 \times 13$	$\sim 20$	$4"\times4"$ square central obscuration

<sup>&</sup>lt;sup>a</sup> Pulnix camera, video frame rate (30 Hz).



An additional use of the acquisition camera will be gathering extrafocal images, which contain information about the second derivative of the wavefront phase across the pupil. These images may be processed with an algorithm similar to the one discussed by Roddier<sup>4,5</sup> to yield a map of the pupil phase itself, providing a useful check and calibration of the AO system, particularly the wavefront sensor.

The steering mirrors SSM1 (a dichroic) and SSM2 are motorized and able to direct light from any chosen guide star onto the wavefront sensor camera under remote control; this steering operation has no effect on the infrared science beam, which passes through the dichroic and is always on-axis.

The wavefront sensor components are mounted on a separate optical breadboard to preserve their internal relative alignment. The guide star light is first collimated and passed through an atmospheric dispersion corrector (ADC) located between the field stop and the Shack-Hartmann lenslet array (LA); the ADC has counter-rotating prisms that are set as a function of telescope zenith angle to introduce a color dispersion opposite to that experienced along the instantaneous line of sight through the atmosphere. This light is then directed onto 4×4-pixel subarrays, one per subaperture in the lenslet array, on the very low-noise, fast-readout CCD of the wavefront sensor camera (WFS CAM). The centroids returned by this array are the basic measurements of the two-dimensional atmospheric phase gradients at a grid of points across the telescope aperture, from which the full aperture phase is reconstructed.

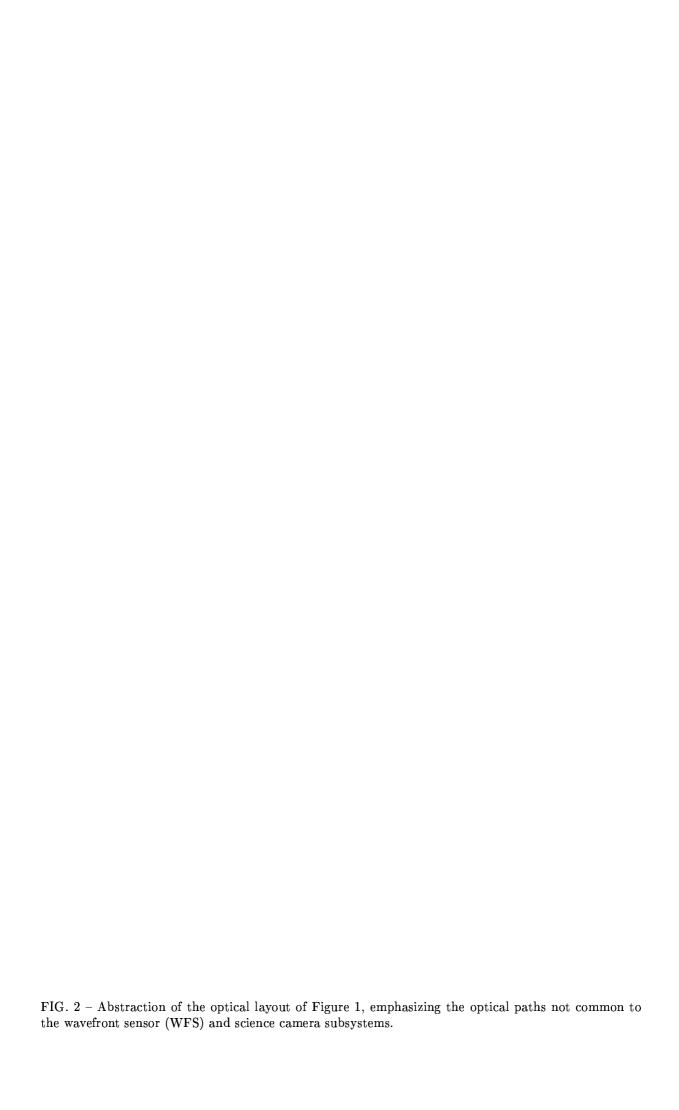
## 3. THE "NON-COMMON" OPTICAL PATHS

Flexure in optical elements upstream of the dichroic will affect the beam reaching the wavefront sensor in the same way as the beam reaching the science camera, and these errors will be automatically corrected when the adaptive optics loop is closed. The effects of such "common-mode" flexures may primarily be described as image motion, and will be handled chiefly in the normal operation of the fast-steering mirror. However, flexure becomes more problematic when it occurs in the dichroic (SSM1) or the optical elements further downstream, where the visible sense beam and the infrared science beam are separated. We refer to these as "non-common paths". Along these paths, deformations due to flexure in the science beam will go undetected by the wavefront sensor and will thus not be corrected, while flexure in the sense beam will have the main effect of causing invalid tip-tilt corrections to be made by the fast-steering mirror, perhaps moving the science beam off the spectrographic slit (with great loss of instrument throughput) or imaging field center (blurring an image).

Our formal design specification for non-common path motion is that it should be controlled or compensated for to a level that results in spot motions on the science camera of no more than 5 milliarc seconds in an hour, or very roughly 10% of the diameter of the Airy disk (the scale of the core of the instrumental point-spread function, ideally, when the adaptive optics system is operating well). This angular scale corresponds to about 2  $\mu$ m of physical spot motion in the f/15.7 science focal plane. At this level, non-common path errors are smaller than anticipated errors of fitting the deformable mirror. It was anticipated during design of the adaptive optics system, however, that focal-plane spot motions of 20 to 100 milliarc seconds due to non-common path flexure might be expected unless some form of metrology were devised to correct for them.

Referring to Figure 2, the chief sources of non-common path flexure are expected to be FM3, SSM1, and SSM2. The several components of the wavefront sensor are compact and mounted together on an optical breadboard to specifically minimize relative flexure and ensure stability to the few-micron level, and the metrology design that we will present later in this paper will rely on this fact. To give an illustrative connection between spot motion and actual tips of optical elements, consider motion of the science spot due to tipping of FM3 in Figure 2. This motion of course goes undetected by the wavefront sensor, but shifts the science beam on the science camera by an amount given by twice the tip angle multiplied by the distance between FM3 and the SCICAM – about 250 mm. A tip of only 10 arc seconds will thus result in a motion of 24  $\mu$ m, exceeding by several times our system specification.

We note in passing that the focussing effects of mirror translation are fairly minor, unlike the spot motions due to mirror translation or to the tip/tilt that we have just discussed. This is because in a slow f/15.7 beam, the focal depth  $\pm$  2 (f/#)<sup>2</sup>  $\lambda$  even at optical wavelengths is still  $\sim \pm$  0.25 mm, and mirror motions this large are not anticipated. (In the infrared beam, tolerances are even more relaxed by a factor of about four).



## 4. FLEXURE DATA IN THE LAB AND AT THE TELESCOPE

An early experimental investigation of flexure in the optical mounts was carried out in the JPL adaptive optics lab. A 6" Aerotech mount of the sort used for several flats in the system, and loaded with a full-weight mirror, was fastened to the optical table and the table was rotated about its long axis. It was found that  $15^{\circ}$  of elevation caused flexures sufficient to deflect the mirror surface by somewhat less than 10". As discussed in the previous section, a tilt of this magnitude at the folding mirror FM3 will cause beam motions at the science camera of about  $24 \mu m$ . Owing to the somewhat longer optical paths, corresponding deviations in the wave-front sensor beam will be somewhat larger if tips in the dichroic (SSM1) or SSM2 are comparable to 10". In another lab test, designed to measure distortion of the optical bench surface, a 10 pound weight was loaded onto an 18 inch mount. Table surface deflections were found to be 20" at a distance of 1 inch from the mount. Hence the mechanical flexures are generally an order of magnitude larger than our specification, and some form of calibration or metrology is needed.

Flexure information has been gathered over the course of initial engineering runs with the adaptive optics system at the 200" telescope, by tracking the motion of guide stars on the science camera and the acquisition camera as the telescope points to different parts of the sky. These data have not yet been fully reduced, but early indications are that the effects of flexure are indeed significant, and that there are preferred directions that dominate image spot motion, corresponding perhaps to preferred flexure of mirror mounts or to the specific bending modes of the optical table. More quantitatively, it appears that at a telescope zenith angle of 15°, image motions of 1/10th of the K-band Airy spot diameter are produced in an exposure time of two minutes...failing to meet our desired specification by roughly an order of magnitude. There is some hope that the preferential direction of the flexure spot motions may be traced to a single inadequate mirror mount, and the problem might be reduced when this mount is reinforced. However, the utility of a real-time metrology system to correct for residual flexure is apparent.

# 5. CORRECTION BY MEASUREMENT OF FLEXURE FOR A GRID OF POINTING POSITIONS

Although laborious, it is straightforward to attempt to account for instrument flexure by measuring it over a systematic grid of telescope pointings, and then applying a correction derived from these measurements to all later observations. This is of course the traditional method used to assess flexure in astronomical instruments or in the telescope itself.

If it is desired to measure flexure over a region of sky down to an angle  $\phi$  away from zenith, with grid spacing  $\Delta\theta$ , then it is necessary to make measurements at a number of points given roughly by

$$N = rac{2\pi[1-cos(\phi)]}{(\Delta heta)^2}$$

where  $\Delta\theta$  must of course be in radians. A reasonable density for sampling the sky would have grid points separated by perhaps 15°. In that case, flexure calibration from zenith down to 60° away from zenith would require measurements at 46 positions. Extending this to 75° would require measurements at 69 positions; the region within 30° from zenith can be calibrated with measurements at only 12 positions. All of these numbers drop as the inverse square of the sample grid spacing angle ( $\Delta\theta=15^\circ$ , e.g.) if sufficient calibration accuracy can be maintained with a coarser grid. It is estimated that each flexure measurement might require a half-minute, while moving the telescope between positions would require a comparable amount of time. So the complete calibration, from zenith down to 60° from zenith, with a 15° grid, would require the better part of an hour to carry out.

The effort necessary to carry out this plan is not excessive, if the flexure corrections thus derived can be counted on to remain constant with time, particularly over the weeks and months of an observing season. However, remapping flexure with each observing run appears to us excessively bothersome and not operationally feasible. Flexure effects might well show variations over short time scales if they are temperature dependent. For the Palomar adaptive optics system, differences in effective flexure with Cassegrain ring angle (azimuthal orientation of the instrument with respect to the telescope) also complicate traditional flexure calibration...that is, the space of possible instrument orientations is now three-dimensional, on the face of it. (It may be hoped that there is no essential dependence on ring angle, and the two degrees of freedom of telescope pointing plus the ring angle degree of freedom might be transformed into just two fundamental variables describing the direction of the gravity vector with respect to the optical bench).

### 6. LASER METROLOGY

An alternative approach favored for our metrology scheme is to monitor the flexure-induced motions of optical elements essentially in real time, by measuring deflections of specially-provided metrology laser beams that are directed onto those elements. Inferring mirror motions or their cumulative effect on science and wavefront-sensing beams with a small number of metrology laser beams can be a subtle problem. We investigated a number of distinctly different schemes, and a few general themes emerged: chief among these, it is important to have the metrology path be as similar as possible to the optical path being monitored. Problems can arise, in particular, when the metrology beam travels in the opposite direction to the beam whose deflections are being monitored. Although the beams suffer the same angular deflection when reflecting off a given mirror with flexure-induced tip or tilt, the difference in propagation path length following the mirror causes the linear spot deflection to be different for the metrology beam. If there are multiple reflections, these differences can be difficult to untangle.

To illustrate the difficulties here, consider a simplified descriptive analysis of an early "straw man" scheme for metrology of the Palomar adaptive optics system. In this plan, a special laser-emitting optical fiber is rigidly mounted in the focal plane of the science camera, offset from the spectrometer slit or imaging-mode field center by an inch or two. Some of the light from this fiber would traverse the infrared path to SSM1 via FM3. Then a special off-axis mirror mounted on the back of SSM1 would divert the metrology beam onto the visible path: from SSM1 to SSM2, through the field stop, which is transparent except for its central 4" patch, and into the acquisition camera. In this way, the metrology beam traverses each of the non-common paths in succession.

Consider first using the same laser-emitting optical fiber in the focal plane of the science camera to undertake the much more modest task of measuring flexure-induced motions in FM3 alone. By operating somewhat off-axis compared to the science beam, it would be possible to position a metrology camera in the vicinity of SSM1 to view the metrology beam. The metrology beam now traverses the same path as the science beam, and responds to deflections of the same mirror, FM3; but the magnitude of the metrology spot deflection will be different from that of the science beam by  $d_1/d_2$ , the ratio of pathlengths after reflection by FM3 ( $d_1 = \text{SSM1} - \text{FM3}$  distance;  $d_2 = \text{SCI CAM} - \text{FM3}$  distance). In this simple case, the mirror deflection or its impact on the science beam could be uniquely extracted by applying the known ratio of pathlengths as a calibration.

The analysis is similar for the single laser metrology beam traversing the infrared and visible non-common paths, as proposed above. Though in some conceptual sense this probe beam is sampling the same mirror deflections as the science and wavefront sensor beams, a more detailed analysis reveals that the quantities that must be measured cannot be deduced from spot deflections of the metrology beam. The deflection of the metrology beam spot is given by a rather complicated expression whose terms include the tip angle of FM3 multiplied by the sum of all the pathlengths from FM3 to the acquisition camera, and the tip angle of SSM1 multiplied by the pathlength from SSM1 to the acquisition camera, and so forth. The full expression is a linear combination of all the tips, tilts, and translations of the elements being monitored, and though the coefficients are known (from the geometry of the optical bench), extraction of the component flexure-induced motions from one measured quantity is not possible. This analysis suggests that simplification is possible only when many terms in the expression for metrology spot deflection are identical or very similar to those for deflection of the adaptive optics system spots...i.e., when the beam paths are identical or very similar, including direction of propagation.

### 7. FAVORED APPROACH: LASER METROLOGY with CORNER CUBE IN COLLIMATED SPACE

The more sophisticated laser metrology scheme that we will describe in this section appears to satisfy the requirements of the Palomar adaptive optics system. Conceptually, it follows the principles discussed in the previous section by effectively injecting the metrology beam upstream of the dichroic, the point at which the non-common paths separate, and ensuring that the beam deflections measured correspond to the same direction of propagation as the adaptive optics beams. It also uses a corner cube to define one non-common path as a reference in a way that allows the use of a single metrology laser beam to monitor both non-common paths (more precisely, it monitors the difference in flexure between these paths, which is all we care about).

The laser source for this scheme is again mounted in the focal plane of the science camera, in a fixed position with respect to the spectroscopic slit or the imaging field center. The path followed by the metrology laser beam is as follows. Referring to Figure 3, consider a corner cube mounted on the periphery of the flat mirror FM2, the first optical element upstream of the dichroic at which the beam from the telescope is collimated. A small amount of light from the laser-emitting optical fiber mounted in the focal plane of the science camera will reach this corner cube by first reflecting from FM3, then passing through the visible-reflecting dichroic SSM1 (with transmission coefficient  $\sim 5\%$ ). The metrology beam then reflects back from the corner cube and the dichroic with high efficiency, and is directed by SSM2 onto an off-axis portion of the acquisition camera (far outside the 4"-diameter zone at the center sending guide star light to the wavefront sensor). Motions of this metrology spot on the acquisition camera, relative to the position of the natural guide star image, will give the excess beam deflection of the visible beam over that of the infrared science beam, and this information will permit the system to hold a science image on the science camera slit or imaging field center to a high degree of accuracy.

To understand the operation of the metrology scheme, consider the propagation of the metrology laser spot with the dichroic (SSM1) removed. The laser is quasi-isotropic, or at least has a large beam, and so some fraction of light emitted from each point on the surface of the fiber output will reach the off-axis paraboloid, OAP2. Since the fiber output is in the science focal plane, OAP2 will collimate the laser light and send it towards FM2. The corner cube on FM2 will retroreflect those rays that it intercepts, and OAP2 will refocus these return rays onto the laser fiber output from which they originated.

Note that this retroreflection to the fiber source is insensitive to a variety of flexure-induced motions in the science path, including tip, tilt, and translation of FM3, and transverse motions of the science camera in the plane perpendicular to the incident science beam. Also, the metrology laser beam provides a reference for the position of the spectroscopic slit or the center of the science image field of view, as appropriate, because its fiber source is rigidly attached to the science focal plane with a known physical offset (1.75 inches at a known angle, in our implementation).

Now we consider operation with the dichroic, SSM1, in place. A small fraction of the retroreflected metrology laser beam still returns to its fiber source in the focal plane of the science camera; however, because of the visible-reflecting nature of the dichroic, most of the returning laser beam is diverted to the acquisition camera. Since the metrology laser source is mounted so far off-axis, the laser beam will pass far from the 4 arc second diameter reflecting spot at the center of the field stop immediately preceding the acquisition camera. As part of the initial setup on a new source, the natural guide star will be steered onto this central spot and will illuminate the wavefront sensor. When the adaptive optic control loop is closed, the position of the guide star will be locked in place by commands derived from the positions of the centroids of the guide star image spots focussed by the 16x16 array of lenslets (subapertures) of the wavefront sensor. Static aberrations within the adaptive optics system optics and the telescope are addressed by having the system drive those centroids not to zero, but to a fixed set of centroid offsets determined through prior system calibration.

As discussed in §3, the positional lock of the natural guide star will tend to compensate for any flexure-induced tips/tilts in the common-path segment of the adaptive optics system, as well as tips and tilts induced by the turbulent atmosphere; of course, the deformable mirror will also make corrections for higher-order atmospheric aberrations. We now consider how to make use of the new element in this scheme: the metrology laser spot on the acquisition camera. This spot provides a reference for the (infrared) science beam in the visible-light, wavefront-sensor portion of the optics. The prescription for using this reference information is fairly intuitive: each wavefront sensor subaperture centroid should have an overall offset added in that will drive the fast-steering mirror (FSM) so as to keep the separation of the natural guide star spot and the metrology laser spot constant. Essentially, this will reverse any differential flexure in the visible and infrared non-common paths, as traced by relative motion of the metrology laser spot and the natural guide star. Instead of holding the natural guide star image "still" on the wavefront sensor camera chip, the natural guide star image is now held still with respect to the metrology laser spot; if there is flexure, this will compensate slow drifts of the science beam from the desired position on the science camera to which it was initially set. The flexure-induced centroid shift will be small, and will move the natural guide star image slightly on the field stop, but not far enough to fall off the 4-arc second reflecting patch.



Illustrating the operation of the new metrology scheme with a case-by-case analysis, flexure in the infrared (science) non-common path will have no effect on the natural guide star image but will move the metrology laser spot on the acquisition camera, and will move the science beam off the slit or imaging center of the science camera. The new adaptive optics control loop proposed here would sense the change in separation of the guide star and metrology laser spots, and would cause an actual (small) movement of the long-term position of the fast-steering mirror (FSM) in a direction that would tend to restore the laser spot to its original position on the acquisition camera...this would have the desired effect of repositioning the science beam onto the science camera slit or field center. If instead we consider the effects of flexure purely in the visible (wavefront sensor) non-common path, the natural guide star beam and the retroreflected laser metrology beam both suffer the same deflections. Hence their separation does not change, and the new control loop takes no action. Indeed, since nothing has happened to divert the science beam from the science camera, no action should be taken to reposition the fast-steering mirror.

The corner cube is injecting a reference spot that is fixed with respect to the desired infrared science beam into the visible-light segment of the adaptive optics system, where the acquisition camera may compare its position to that of the natural guide star from which the wavefront sensor is deriving tip/tilt corrections, and make small flexure amendments to those corrections. Errors due to the dissimilar paths followed by the metrology beam and the non-common path beams will be proportional to the cosine of the (small) angles between those beams. For the physical dimensions of our adaptive optics system and the linear offset of the metrology laser source fiber, those angles are at most roughly 5°. Owing to the retroreflecting properties of the corner cube, the metrology scheme presented here is quite insensitive to positioning of the corner cube itself or flexure in its mount.

## 8. LASER METROLOGY SIGNAL STRENGTH, SPOT SIZE

A natural concern in this scheme is the brightness of the laser metrology spot on the acquisition camera, since it must pass the "wrong way" through the visible-reflecting dichroic SSM1 before reaching OAP2 and the corner cube. Flux calculations through the entire metrology path confirm, however, that the laser power available for detection is adequate. The metrology laser emits a power output of  $100~\mu$ Watts into a beam at roughly f/5 (and hence solid angle of about  $\Omega \sim 1/25$  sr). At the wavelength of a HeNe laser, the dichroic transmission is about 0.05; so only 0.95 gets reflected on the return leg of the metrology path, but we will ignore this and other reflection losses on the level of a few percent. The metrology beam expands until it hits OAP2, which is about 68 inches from the science camera focal plane. All rays that intercept the corner cube of diameter  $D_{cc}$  will be retroreflected and sent back to the image of the laser-emitting optical fiber, which is now in the acquisition camera focal plane since the rays have been diverted by the dichroic. Putting these factors together, the power delivered to the spot in the acquisition camera is

$$P_{acq} \sim (100~\mu Watts) \times 0.05 \times \frac{1}{\Omega} (\frac{D_{cc}}{68~inches})^2 \sim 3 \times 10^{-8}~Watts$$

which is  $9 \times 10^{10}$  photons per second for a 1"-diameter corner cube ( $D_{cc} = 1$  inch). This appears to be plenty of photon flux for a determination of the centroid of the metrology laser spot.

Also of concern is the size of the metrology laser spot in relation to the pixel scale of the acquisition camera, and the expected magnitude of spot motions that would correspond to the level of flexure metrology desired. Owing to the proximity of the Nikon lens to the acquisition camera, there is a large demagnification of the metrology laser beam (by a factor of roughly  $\sim 7.6$ ). Hence the metrology spot size, which was originally the 50  $\mu$ m diameter of the launching fiber output in the focal plane of the science camera, is now only about 6.6  $\mu$ m, and the flexure motions that correspond to motions of 2 or 3  $\mu$ m in that focal plane would be demagnified to only  $\sim 0.3$   $\mu$ m on the acquisition camera. Since the acquisition camera has 11x13  $\mu$ m pixels, some auxiliary scheme for imaging the metrology laser spot appears necessary; the beam is in any case vignetted by the Nikon lens holder in the current configuration. An additional Pulnix camera is available for metrology spot imaging. Some additional care will be taken in installating it to ensure the rigidity of the camera used for metrology spot imaging with respect to the wavefront sensor optical breadboard, as the field stop is part of that breadboard but the current acquisition camera is not.

## 9. CONCLUSIONS

It is apparent that the dramatic reduction in scale of the point-spread function in an adaptive optics system makes flexure-induced motions of optical elements particularly deleterious to system operation. The elements whose motions have the most impact are those in the "non-common" optical paths, downstream from the dichroic that separates light going to the science camera from light going to the wavefront sensor. We have presented here the initial conceptual design of a simple but effective real-time laser metrology system designed specifically to monitor the effects of non-common path flexure. Referring to Figure 3, this system promises to allow compensation for all of the sources of non-common path flexure that are expected to be most problematic: tips, tilts, and translations of FM3, SSM1, and SSM2, and transverse translations of the science camera and of the optical breadboard housing the wavefront sensor.

If the efficacy of the design presented here is verified by more detailed raytracing studies and by subsequent laboratory tests, it might prove to be a useful addition to any of a broad class of adaptive optics systems similar to our fairly standard design.

### 10. ACKNOWLEDGMENTS

The JPL adaptive optics team includes Gary Brack, Ben Oppenheimer, Dean Palmer, and Kent Wallace, and many helpful ideas have been contributed by Mark Colavita and Mike Shao.

#### 11. REFERENCES

- 1. H. W. Babcock, "The Possibility of Compensating Astronomical Seeing", Pub. Astron. Soc. Pac., vol. 65, pp. 229-236, 1953.
- 2. see Adaptive Optics, Vol. 13, 1996 OSA Technical Digest Series (Optical Society of America, Washington, DC, 1996), and references therein.
- 3. R. G. Dekany, "The Palomar Adaptive Optics System", in *Adaptive Optics*, Vol. 13, 1996 OSA Technical Digest Series (Optical Society of America, Washington, DC, 1996), pp. 40-42.
- 4. F. Roddier, "Curvature Sensing and Compensation: A New Concept in Adaptive Optics", *Appl. Opt.*, vol. 27, pp. 1223-1225, 1988.
- 5. F. Roddier, M. Northcott, and J. E. Graves, "A Simple Low-order Adaptive Optics System for Near-infrared Applications", *Pub. Astron. Soc. Pac.*, vol. 103, pp. 131-149, 1991.